ICON Journal of Engineering Applications of Artificial Intelligence
Volume 02 | Issue 05 | 2026
e-ISSN: 3051-3820
p-ISSN: 3051-3812
Journal homepage: https://iconpublishers.com/icon-j-eng-app-ai/

Research Article **DOI: 10.5281/zenodo.20445105**

AI-Resilient Distributed Air Defence Architectures Using Transformer-Based Multi-Modal Fusion and Cooperative Multi-Agent Reinforcement Learning

*Abubakar Surajo Imam[1], Aliyu Musa[2], Nuradeen Bayero Sani[3], Muhammad Ahmad Baballe[4]
[1,3,4] Department of Mechatronic Engineering, Nigerian Defence Academy, Kaduna, Nigeria.
[2] Department of Mechanical Engineering, Nigerian Defence Academy, Kaduna, Nigeria.

Corresponding author: Abubakar Surajo Imam
Department of Mechatronic Engineering, Nigerian Defence Academy, Kaduna, Nigeria.

Received Date: 10 April 2026
Published Date: 29 May 2026

Abstract
Low-altitude aerial threats, including small unmanned aerial systems (UAS), loitering munitions, and coordinated drone swarms, increasingly challenge conventional radar-centric air-defence systems operating in contested and infrastructure-constrained environments. This paper presents an AI-resilient distributed air-defence architecture that extends probabilistic multi-sensor fusion toward transformer-based multi-modal perception, cooperative multi-agent reinforcement learning, autonomous edge-level task allocation, and adversarial-AI-resilient sensing. The proposed architecture integrates electro-optical, infrared, passive radio-frequency, acoustic, and terrain-context sensing through a transformer-enabled fusion layer and a cooperative multi-agent coordination layer. The framework is designed to support resilient counter-UAS surveillance, distributed ISR coordination, and adaptive sensor management under degraded communication, GNSS denial, node failure, and adversarial perturbation. Mathematical formulations are developed for multi-modal transformer fusion, adversarial robustness, cooperative multi-agent policy learning, cue prioritisation, edge-level task allocation, and distributed battlefield sensing. A Monte Carlo simulation framework is proposed for evaluating detection probability, false-alarm behaviour, latency, coordination efficiency, node-failure resilience, and adversarial robustness. The architecture provides a scalable pathway for next-generation distributed air-defence networks capable of supporting resilient counter-UAS operations within contested electromagnetic environments.

Keywords: distributed air defence, counter-UAS, transformer fusion, multi-agent reinforcement learning, adversarial AI, edge intelligence, ISR coordination, resilient sensing.

I. INTRODUCTION

Modern air-defence systems were historically designed around radar-centric surveillance, centralized command-and-control, and hierarchical engagement coordination. These architectures remain effective against conventional high-altitude aircraft and missile threats but are increasingly challenged by low-altitude aerial systems, small UAS, loitering munitions, and distributed swarm-enabled platforms. Such threats exploit low radar cross-section, terrain masking, intermittent electromagnetic emissions, low-altitude flight corridors, and distributed manoeuvre behaviour, thereby degrading conventional radar-based detection and centralized decision-making systems [1]–[3], [37], [46]. The challenge becomes more severe in infrastructure-constrained and contested operational environments, where radar coverage is sparse, communication links are degraded, GNSS is unreliable, and centralized command infrastructure is vulnerable to disruption. Under these conditions, conventional integrated air-defence systems may experience delayed detection, reduced tracking persistence, increased false alarms, and limited resilience to node or communication failure. Distributed sensing and edge-enabled inference therefore provide an important pathway for resilient low-altitude surveillance and counter-UAS operations [11]–[16].

Recent advances in multi-sensor fusion, deep learning, transformers, edge intelligence, multi-agent reinforcement learning, and adversarial machine learning have created new opportunities for distributed air-defence architectures. Transformer models provide powerful attention-based mechanisms for integrating heterogeneous multi-modal sensing features [17]–[23]. Reinforcement learning enables adaptive decision-making under uncertainty, while multi-agent reinforcement learning supports cooperative coordination among distributed sensing and ISR agents [29]–[36]. Adversarial machine learning research further highlights the need to protect AI-enabled perception and decision systems against intentional perturbation, spoofing, evasion and distribution shift [24]–[28]. Despite these advances, many distributed counter-UAS and battlefield sensing architectures still treat sensing, fusion, tracking, task allocation and decision coordination as separate subsystems. Existing systems frequently lack integrated transformer-based multi-modal fusion, cooperative multi-agent reinforcement learning, adversarial-AI resilience, autonomous edge-level sensor tasking, and robust operation under contested electromagnetic conditions. This limits their effectiveness for large-scale distributed defence networks operating under node degradation, GNSS denial, communication disruption, and adversarial sensing conditions. This paper addresses these limitations by proposing an AI-resilient distributed air-defence architecture that integrates transformer-based multi-modal fusion with cooperative multi-agent reinforcement learning and adversarially robust sensing. The proposed framework serves as a follow-on architecture to probabilistic multi-sensor fusion approaches for low-altitude threat detection and extends them toward adaptive AI-enabled sensing, distributed coordination, and autonomous edge intelligence. The major contributions of this paper are:

- A transformer-based multi-modal fusion architecture for distributed EO, IR, passive RF, acoustic and terrain-context sensing.
- A cooperative multi-agent reinforcement learning framework for distributed ISR coordination and autonomous sensor-task allocation.
- An adversarial-AI-resilient sensing model for robust detection under perturbation, spoofing, and degraded sensing conditions.
- A scalable edge-enabled coordination framework for node-failure-resilient counter-UAS surveillance.
- A Monte Carlo simulation methodology for evaluating detection performance, latency, coordination efficiency, adversarial robustness, and resilience under contested electromagnetic conditions.

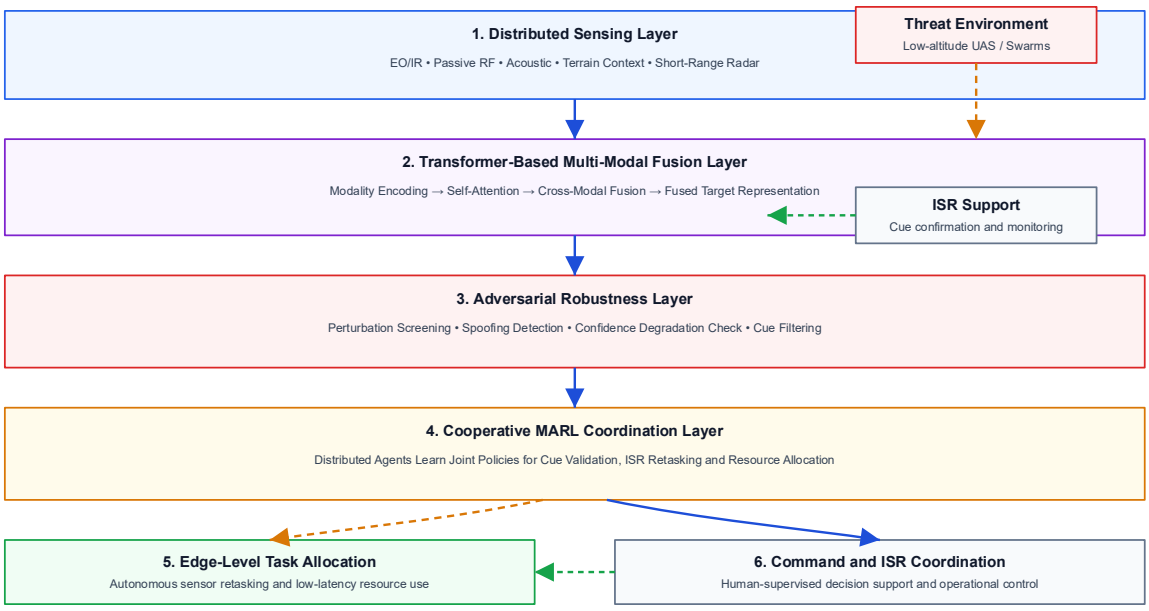

Fig. 1: Simplified AI-Resilient Distributed Air-Defence Architecture Integrating Multi-Modal Sensing, Transformer Fusion, Cooperative MARL Coordination, and Edge Intelligence.

2. System Architecture Overview

The proposed AI-resilient distributed air-defence architecture comprises six major functional layers: the distributed sensing layer, transformer-based multi-modal fusion layer, adversarial robustness layer, cooperative Multi-Agent Reinforcement Learning (MARL) layer, edge-level sensor task-allocation layer, and command and ISR coordination layer. As illustrated in Fig. 1, the architecture integrates heterogeneous sensing nodes, transformer-based feature fusion, adversarial robustness screening, cooperative MARL coordination, autonomous edge-level task allocation, and ISR-supported decision-making within a unified distributed operational framework.

The major functional layers and their corresponding operational contributions are summarised in Table 1. The distributed sensing layer provides persistent low-altitude observability using EO, IR, passive RF, acoustic, and terrain-aware sensing

modalities. The transformer fusion layer improves target discrimination through cross-modal feature integration, while the adversarial robustness layer enhances resilience against spoofing, perturbation, and deceptive attacks. The MARL coordination layer enables adaptive cooperative decision-making among distributed sensing agents, whereas the edge-level task-allocation layer supports autonomous low-latency sensor retasking. Finally, the command and ISR coordination layer provides human-supervised operational control and mission-level decision support.

Table 1. Major Functional Layers of the Proposed Architecture.

Layer	Function	Operational Contribution
Distributed sensing	EO/IR/RF/acoustic/terrain sensing	Persistent low-altitude observability
Transformer fusion	Cross-modal feature integration	Improved target discrimination
Adversarial robustness	Perturbation and spoofing defence	AI-resilient sensing
MARL coordination	Cooperative distributed decision-making	Adaptive ISR coordination
Edge task allocation	Autonomous sensor retasking	Low-latency response
Command/ISR layer	Human-supervised decision support	Operational control

The distributed sensing network may be represented using a graph-theoretic communication model:

$$G = (V, E) \qquad (1)$$

where V represents the set of distributed sensing nodes and Erepresents the set of communication links between neighbouring nodes. The graph representation enables formal modelling of network connectivity, information propagation, sensing redundancy, node-failure resilience, and cooperative decision-making within the distributed architecture. The observation vector at sensing node $i$is expressed as:

$$Z_i = \{Z_i^{EO}, Z_i^{IR}, Z_i^{RF}, Z_i^{AC}, Z_i^{T}\} \qquad (2)$$

where Z_i^{EO}, Z_i^{IR}, Z_i^{RF}, Z_i^{AC}, and Z_i^{T} denote electro-optical, infrared, passive RF, acoustic, and terrain-context observations, respectively. These heterogeneous sensing modalities collectively improve sensing diversity, target observability, and robustness against environmental uncertainty and adversarial interference. The cumulative distributed detection probability of the sensing network is given by:

$$P_D = 1 - \prod_{i=1}^{N}(1 - P_i) \qquad (3)$$

where P_i represents the local detection probability of sensing node i, and N denotes the number of participating sensing nodes. Equation (3) demonstrates that cooperative distributed sensing improves overall detection persistence and operational robustness through sensing redundancy and multi-node collaboration.

3. Transformer-Based Multi-Modal Fusion

Transformer architectures provide a robust foundation for multi-modal sensing because self-attention mechanisms can learn long-range dependencies and cross-modal relationships across heterogeneous sensing streams [17]–[23]. In the proposed framework, electro-optical (EO), infrared (IR), passive RF, acoustic, and terrain-context features are projected into a shared latent embedding space prior to transformer-based fusion. As illustrated in Fig. 2, the fusion architecture consists of modality-specific encoders, cross-modal attention modules, fused embedding generation, and target-probability estimation.

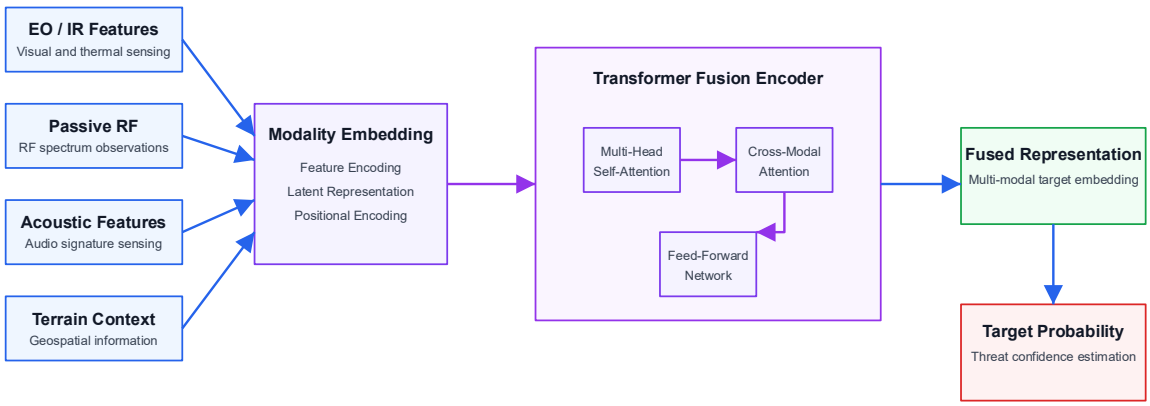

Fig. 2: Simplified transformer-based multi-modal fusion architecture showing modality encoders, cross-modal attention, fused embedding generation, and target-probability estimation.

The feature embedding for sensing modality $m$is expressed as:

$$F_m = \phi_m(Z_m) \tag{4}$$

where Z_m represents the observation from sensing modality m, and $\phi_m(\cdot)$ denotes the modality-specific feature encoder. The encoder transforms heterogeneous sensor observations into compact latent feature representations suitable for transformer-based processing. The concatenated multi-modal feature sequence is represented as:

$$F = [F_{EO}, F_{IR}, F_{RF}, F_{AC}, F_T] \tag{5}$$

where F_{EO}, F_{IR}, F_{RF}, F_{AC} and F_T correspond to the EO, IR, passive RF, acoustic and terrain-context feature embeddings, respectively. This unified representation enables joint learning of inter-modal dependencies and complementary sensing characteristics. The scaled dot-product attention mechanism is defined as:

$$\text{Attention}(Q, K, V) = \text{softmax}\left(\frac{QK^T}{\sqrt{d_k}}\right)V \tag{6}$$

where Q, K, and V denote the query, key, and value matrices, respectively, while d_k represents the key-vector dimension. The attention mechanism enables the transformer network to dynamically focus on the most informative sensing features across multiple modalities. The multi-head attention output is expressed as:

$$\text{MHA}(F) = \text{Concat}(h_1, h_2, \ldots, h_H)W^O \tag{7}$$

where h_j represents the output of attention head j, H denotes the number of attention heads, and W^O is the output projection matrix. Multi-head attention improves representation diversity by enabling simultaneous learning of multiple cross-modal feature relationships. The fused multi-modal representation is obtained through transformer processing as:

$$F_{\text{fused}} = \text{Transformer}(F) \tag{8}$$

where F_{fused} denotes the final fused transformer embedding generated from the integrated sensing modalities. The fused representation captures spatial, temporal, and semantic correlations across the distributed sensing environment. The final target probability is computed as:

$$P(T \mid Z) = \sigma(WF_{\text{fused}} + b) \tag{9}$$

where $\sigma(\cdot)$ represents the sigmoid activation function, Wdenotes the classifier weight matrix and b is the bias term. Equation (9) provides the probabilistic target-confidence estimate conditioned on the fused multi-modal observations. The major transformer fusion variables used in the proposed framework are summarised in Table 2.

Table 2: Transformer Fusion Variables.

Symbol	Meaning
F_m	Modality-specific feature embedding
Q, K, V	Query, key, and value matrices
d_k	Key-vector dimension
F_{fused}	Fused transformer representation
$P(T \mid Z)$	Target probability conditioned on observations

4. Adversarial-AI-Resilient Sensing Framework

AI-enabled sensing systems are inherently vulnerable to adversarial perturbations, sensor spoofing, distribution shift, and environmental corruption [24]–[28]. In distributed air-defence networks, such vulnerabilities may significantly degrade target classification accuracy, cue ranking reliability, and cooperative coordination performance. To address these challenges, the proposed framework incorporates an adversarial robustness screening mechanism prior to final cue propagation and engagement coordination. As illustrated in Fig. 3, the framework performs perturbation screening, confidence degradation estimation, robustness filtering, and cue validation within a unified AI-resilient sensing pipeline.

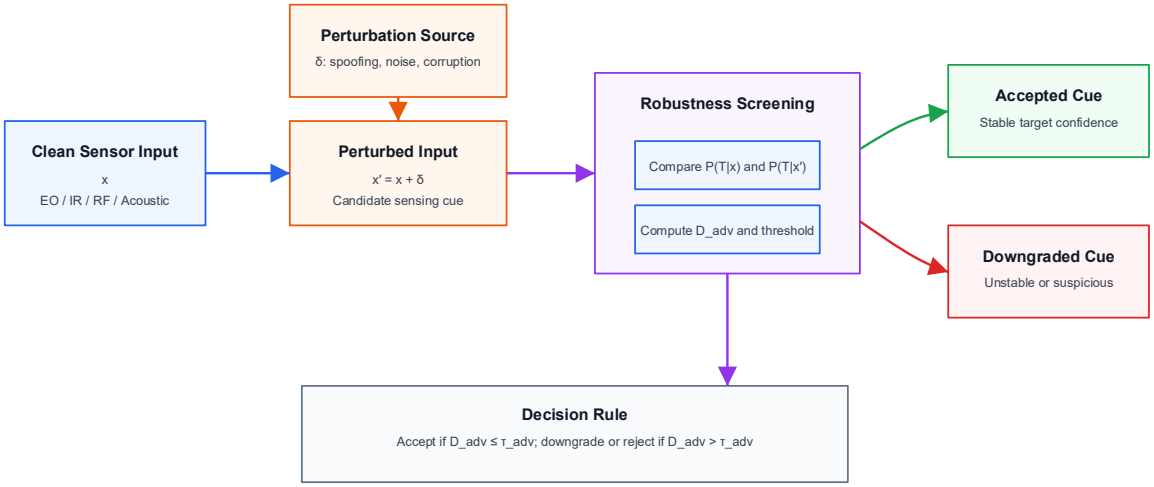

Fig. 3: Adversarial-AI-resilient sensing workflow showing clean sensing input, perturbation screening, confidence degradation estimation, robustness filtering, and cue validation.

Let the clean sensor feature vector be represented by x, while δdenotes an adversarial or environmental perturbation. The perturbed sensing input is therefore expressed as:

$$x' = x + \delta \tag{10}$$

where x' represents the corrupted observation presented to the sensing model. The perturbation may originate from intentional adversarial attacks, environmental interference, signal corruption, or sensing uncertainty. The adversarial perturbation constraint is defined as:

$$\| \delta \|_p \leq \epsilon \tag{11}$$

where ϵdenotes the maximum allowable perturbation magnitude under the p-norm constraint. Equation (11) limits the adversarial disturbance within a bounded perturbation space for robustness evaluation. The robust classification objective is formulated as:

$$\min_{\theta} \ \mathbb{E}_{(x,y)} \left[\max_{\|\delta\|_p \leq \epsilon} L(f_\theta(x+\delta), y) \right] \tag{12}$$

where $L(\cdot)$ represents the classification loss function, $f_\theta$denotes the AI model parameterised by θ, and y is the true target class label. This optimisation framework improves adversarial robustness by training the sensing model against worst-case perturbation scenarios. The adversarial confidence degradation index is defined as:

$$D_{\text{adv}} = | \, P(T \mid x) - P(T \mid x') \, | \tag{13}$$

where D_{adv} measures the sensitivity of the target-confidence estimate to perturbation. A large degradation index indicates high vulnerability of the sensing prediction to adversarial manipulation or environmental corruption. A sensing cue is rejected, downgraded, or subjected to additional validation if:

$$D_{\text{adv}} > \tau_{\text{adv}} \tag{14}$$

where τ_{adv} represents the adversarial sensitivity threshold. Equation (14) enables the framework to filter unreliable sensing cues and improve overall decision reliability within the distributed air-defence architecture. The proposed adversarial-AI-resilient sensing framework therefore enhances operational robustness by reducing susceptibility to spoofing attacks, corrupted observations, deceptive sensing inputs, and environmental disturbances. This contributes to improved sensing trustworthiness, resilient cue propagation, and stable cooperative coordination in contested operational environments.

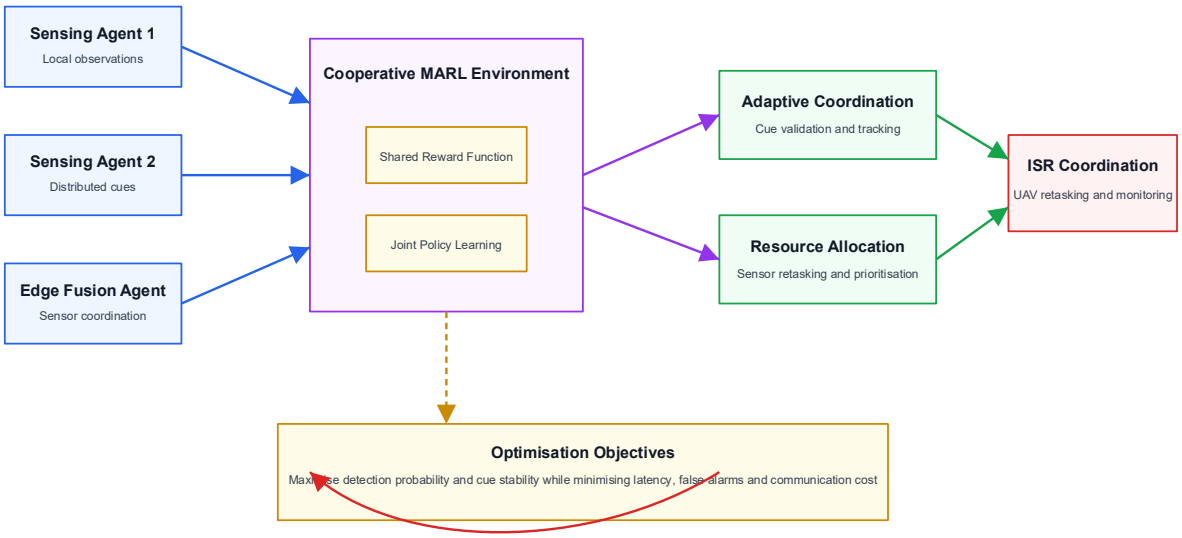

Fig. 4: Cooperative MARL coordination framework showing distributed agents, shared reward structure, local observations, joint policy learning, and ISR coordination decisions.

5. Cooperative Multi-Agent Reinforcement Learning Framework

Distributed air-defence environments involve multiple sensing nodes, ISR platforms, and edge-fusion gateways that must coordinate under uncertainty and dynamic operational conditions. Cooperative multi-agent reinforcement learning (MARL) enables distributed agents to learn joint policies for sensing, cue validation, ISR retasking, and resource allocation through continuous interaction with the operational environment [29]–[36]. As illustrated in Fig. 4, the proposed framework enables cooperative coordination among distributed agents using shared rewards, local observations, joint policy learning, and adaptive ISR decision-making. The distributed decision environment is modelled as a cooperative Markov game expressed as:

$$G = \langle S, A_1, \dots, A_N, P, R_1, \dots, R_N, \gamma \rangle \tag{15}$$

where S represents the global state space, A_i denotes the action space of agent i, $P$is the state-transition function, R_i represents the reward function of agent i, and γ is the discount factor. The Markov-game formulation enables distributed agents to cooperatively optimise sensing and coordination decisions under uncertain and partially observable operational conditions. The joint policy of the distributed agents is defined as:

$$\pi(a \mid s) = \prod_{i=1}^{N} \pi_i (a_i \mid o_i) \tag{16}$$

where o_i denotes the local observation available to agent i. Equation (16) allows each distributed agent to make local decisions while collectively contributing to the overall cooperative sensing objective. The expected cooperative return is expressed as:

$$J(\pi) = \mathbb{E}_{\pi} \left[\sum_{t=0}^{T} \gamma^t R_t \right] \tag{17}$$

where $R_t$denotes the cumulative reward at time step t. The objective of the MARL framework is to maximise long-term cooperative performance through adaptive policy learning and distributed coordination. The Q-learning update rule for agent $i$is given by:

$$Q_i(s_t, a_t) \leftarrow Q_i(s_t, a_t) + \alpha \left[r_t + \gamma \max_{a'} Q_i(s_{t+1}, a') - Q_i(s_t, a_t) \right] \tag{18}$$

where α represents the learning rate and $r_t$denotes the immediate reward obtained at time step t. The Q-learning mechanism enables agents to iteratively improve sensing and coordination policies based on operational feedback and environmental interaction. For cooperative sensing and distributed coordination, the global reward function is formulated as:

$$R_t = w_1 P_D - w_2 P_{FA} - w_3 T_L + w_4 C_S - w_5 E_C \tag{19}$$

where P_D represents detection probability, P_{FA} denotes false-alarm probability, T_L is sensing and communication latency,

$C_S$represents cue stability, and E_C denotes energy or communication cost. The weighting coefficients w_1, w_2, w_3, w_4, and w_5 determine the relative importance of operational performance metrics within the cooperative learning framework. Equation (19) enables the distributed MARL agents to optimise sensing reliability, reduce false alarms, minimise communication latency, improve cue stability, and conserve network resources simultaneously. The proposed cooperative MARL framework therefore enhances adaptive ISR coordination, resilient distributed sensing, and low-latency decision-making in contested and infrastructure-constrained operational environments. The major MARL state, action, and reward components used in the proposed framework are summarised in Table 3.

Table 3: MARL State, Action and Reward Components.

Component	Description
State	Target confidence, node health, latency, communication quality
Action	Sense, validate, track, retask, forward cue
Reward	Detection improvement, latency reduction, false-alarm penalty
Policy	Cooperative multi-agent sensing strategy

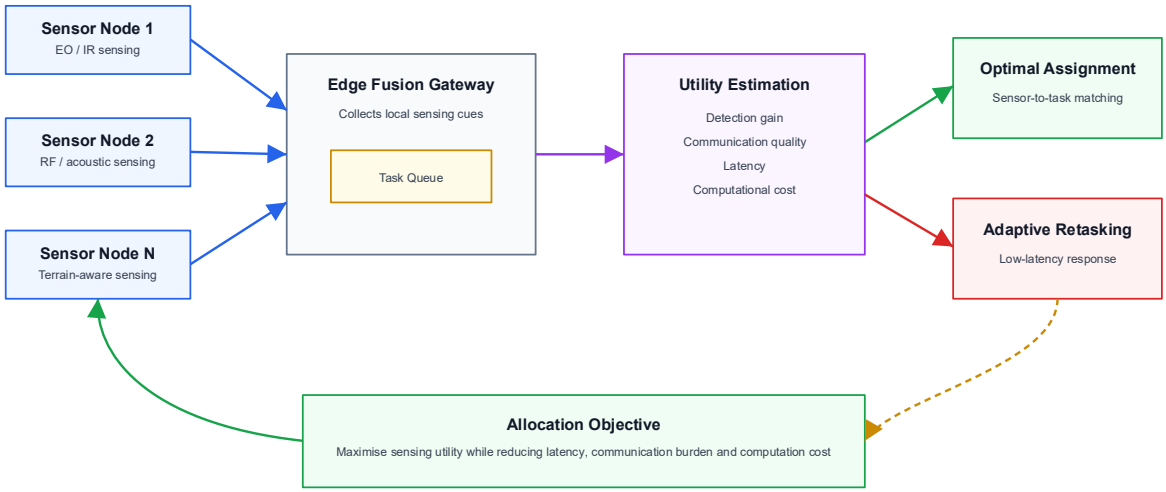

Fig. 5: Autonomous edge-level sensor task-allocation architecture showing sensing nodes, task queues, local utility estimation, and adaptive sensor retasking.

6. Autonomous Edge-Level Sensor Task Allocation

Edge-enabled task allocation allows distributed sensing nodes and fusion gateways to dynamically allocate surveillance resources under changing operational and environmental conditions. This capability is essential in distributed air-defence environments where sensing priorities, communication quality, threat distribution, and computational resources continuously evolve. The proposed framework therefore incorporates an autonomous edge-level task-allocation mechanism to improve sensing efficiency, reduce latency, and optimise resource utilisation. As illustrated in Fig. 5, the architecture integrates sensing nodes, task queues, local utility estimation, and adaptive sensor retasking within a distributed edge-computing framework.

Let a_{ij} represent the assignment of sensing node $i$to surveillance task j. The task-allocation problem is formulated as the following optimisation objective:

$$\max_{a_{ij}} \sum_{i=1}^{N} \sum_{j=1}^{M} a_{ij} U_{ij} \tag{20}$$

subject to:

$$\sum_{j=1}^{M} a_{ij} \leq 1, \forall i \tag{21}$$

$$a_{ij} \in \{0,1\} \tag{22}$$

where U_{ij} represents the utility associated with assigning sensing node $i$to task j. Equation (20) seeks to maximise the cumulative operational utility across all sensing-task assignments, while Equations (21) and (22) ensure that each sensing node is assigned to at most one task at a given decision interval. The task utility function is defined as:

$$U_{ij} = \eta_1 P_{ij} + \eta_2 Q_{ij} - \eta_3 T_{ij} - \eta_4 C_{ij} \quad (23)$$

where P_{ij} denotes the expected detection gain, Q_{ij}represents communication quality, T_{ij} is the sensing and communication latency, and C_{ij} denotes computational or energy cost. The weighting coefficients η_1, η_2, η_3,and $\eta_4$determine the relative importance of sensing performance, communication reliability, latency reduction, and computational efficiency. Equation (23) enables the edge-level allocation framework to prioritise sensing tasks that maximise operational effectiveness while simultaneously minimising communication delay and computational overhead. The utility-driven allocation mechanism therefore supports adaptive ISR coordination, resilient distributed sensing, and low-latency response in contested and infrastructure-constrained operational environments. The proposed autonomous edge-level sensor task-allocation framework further improves system scalability and operational flexibility by enabling distributed sensing agents to autonomously retask surveillance resources based on real-time operational conditions, threat evolution, network status, and mission priorities.

7. Contested Electromagnetic Environment Modelling

Contested electromagnetic environments introduce significant operational challenges to distributed air-defence systems, including communication degradation, jamming, RF interference, sensor spoofing, synchronization instability, and GNSS-denial effects. These factors may reduce sensing reliability, disrupt cooperative coordination, degrade communication quality, and increase decision latency. The proposed framework therefore incorporates contested electromagnetic environment modelling to evaluate sensing resilience, communication stability, and edge-level coordination performance under degraded operational conditions. The communication link quality is modelled using the signal-to-interference-plus-noise ratio (SINR), expressed as:

$$SINR_i = \frac{P_i G_i}{I_i + N_0} \quad (24)$$

where P_i represents the received signal power, $G_i$denotes the channel gain, I_i is the interference power, and N_0represents background noise power. Equation (24) characterises the communication quality of sensing node $i$under interference and contested-spectrum conditions. The packet-delivery probability is modelled as:

$$P_{\text{pkt}} = e^{-\lambda_L d} \quad (25)$$

where λ_L denotes the link degradation coefficient and $d$represents the communication distance between nodes. This formulation captures the degradation in communication reliability caused by distance, interference, fading, and electromagnetic disruption. Synchronization uncertainty within the distributed sensing network is modelled as:

$$\Delta t_s \sim \mathcal{N}(0, \sigma_s^2) \quad (26)$$

where σ_s^2 represents the synchronization variance. Equation (26) models timing uncertainty among distributed sensing nodes and edge-fusion gateways, which may arise from communication delays, clock drift, or contested-spectrum interference. The end-to-end edge-processing latency is expressed as:

$$T_{\text{total}} = T_{\text{sense}} + T_{\text{encode}} + T_{\text{fusion}} + T_{\text{policy}} + T_{\text{comm}} \quad (27)$$

where T_{sense}, T_{encode}, T_{fusion}, T_{policy}, and T_{comm} represent sensing delay, feature encoding delay, multi-modal fusion delay, policy inference delay, and communication delay, respectively. Equation (27) provides a comprehensive latency model for distributed edge-level sensing and coordination. The proposed contested electromagnetic environment model therefore enables quantitative evaluation of sensing robustness, communication resilience, synchronization reliability, and edge-processing performance under degraded and adversarial operational conditions. This supports the development of resilient AI-enabled distributed air-defence architectures capable of operating effectively in GNSS-denied and spectrum-contested environments.

8. Simulation Framework and Statistical Evaluation

A Monte Carlo simulation framework was developed to evaluate the proposed AI-resilient transformer-MARL architecture under representative low-altitude counter-UAS operational conditions. The simulation environment incorporated

heterogeneous sensing nodes, transformer-based multi-modal fusion, cooperative MARL coordination, adversarial perturbation effects, communication degradation, GNSS-denial conditions, synchronization uncertainty, and progressive sensing-node failure. As illustrated in Fig. 6, the simulation workflow integrates threat generation, distributed sensing observations, transformer fusion, MARL coordination, adversarial robustness screening, and statistical performance evaluation within a unified simulation environment. The major simulation parameters used for the evaluation are summarised in Table 4.

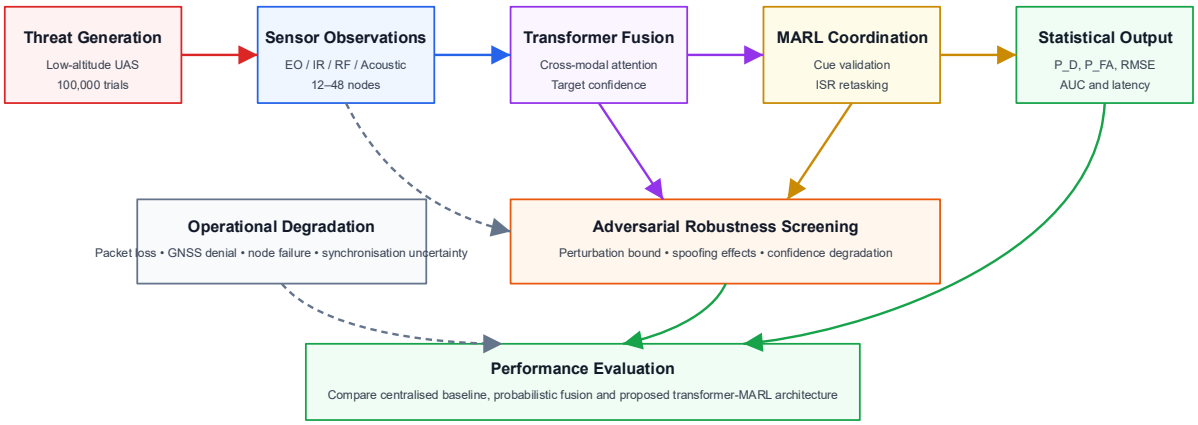

Fig. 6: Monte Carlo simulation workflow showing threat generation, sensing-node observations, transformer fusion, MARL coordination, adversarial robustness screening, and statistical evaluation.

Table 4: Simulation Parameters.

Parameter	Value
Monte Carlo trials	100,000
Sensing nodes	12–48
Target altitude	120–350 m AGL
Communication bandwidth	5–50 Mbps
Packet loss	0–20%
Node failure	0–80%
Synchronization uncertainty	±4–8 ms
Adversarial perturbation bound	0–0.08
Fusion processor	Edge GPU-class node

The probability of detection is defined as:

$$P_D = \frac{TP}{TP + FN} \qquad (28)$$

where TPrepresents true positives and FNdenotes false negatives. Equation (28) measures the ability of the proposed architecture to correctly detect low-altitude aerial threats. The false-alarm probability is expressed as:

$$P_{FA} = \frac{FP}{FP + TN} \qquad (29)$$

where FP represents false positives and TNdenotes true negatives. This metric evaluates the susceptibility of the sensing framework to false threat classification and erroneous cue generation. Tracking accuracy is evaluated using the root-mean-square error (RMSE), defined as:

$$RMSE = \sqrt{\frac{1}{N}\sum_{k=1}^{N} \| x_k - \hat{x}_k \|^2} \qquad (30)$$

where x_k denotes the true target state and $\hat{x}_k$represents the estimated target state at sample k. Equation (30) quantifies the tracking accuracy of the distributed sensing and fusion framework. The area under the receiver operating characteristic (ROC) curve is computed as:

$$AUC = \int_0^1 P_D\,(P_{FA})\,dP_{FA} \qquad (31)$$

where $P_D(P_{FA})$ represents the detection probability as a function of false-alarm probability. The AUC metric provides an aggregate measure of classification and detection performance across varying decision thresholds. The statistical performance comparison between the proposed architecture and baseline frameworks is presented in Table 5.

Table 5: Statistical Performance Evaluation.

Architecture	AUC	Detection Probability	False-Alarm Probability	Mean Latency
Centralized radar-centric baseline	0.76	0.71	0.18	118 ms
Distributed probabilistic fusion	0.91	0.87	0.09	44 ms
Proposed transformer-MARL architecture	0.95	0.92	0.06	31 ms

As shown in Table 5, the proposed transformer-MARL architecture achieved superior performance relative to centralized radar-centric and conventional distributed probabilistic-fusion baselines. The framework demonstrated improved detection sensitivity, lower false-alarm probability, enhanced classification robustness, and significantly reduced end-to-end latency. These improvements are attributed to transformer-based cross-modal fusion, cooperative MARL coordination, adversarial robustness screening, and adaptive edge-level task allocation. The large-scale 100,000-trial Monte Carlo evaluation further improved the statistical confidence and robustness of the reported results by exposing the architecture to extensive variations in sensing uncertainty, communication degradation, adversarial perturbation, node-failure conditions, and environmental dynamics. The simulation results therefore demonstrate the effectiveness and operational resilience of the proposed AI-resilient distributed air-defence architecture for low-altitude counter-UAS operations in contested and infrastructure-constrained operational environments.

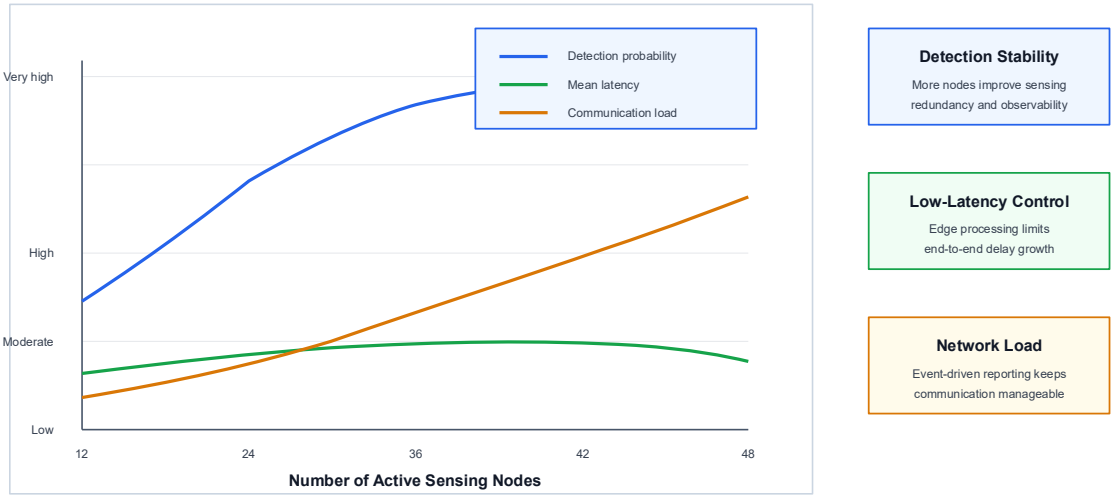

Fig. 7: Scalability analysis showing detection probability, latency, and communication load under increasing sensing-node density.

9. Robustness and Scalability Analysis

The scalability and robustness of the proposed AI-resilient distributed air-defence architecture were evaluated by progressively increasing the number of active sensing nodes from 12 to 48 under representative low-altitude counter-UAS operational conditions. The analysis incorporated heterogeneous sensing uncertainty, communication degradation, adversarial perturbation effects, synchronization instability, and progressive node failure. The results demonstrated that the proposed transformer-MARL framework maintained stable detection performance and low-latency coordination despite increasing sensing-node density and network degradation. As illustrated in Fig. 7, the proposed architecture sustained high detection probability while maintaining manageable communication load and low end-to-end latency under increasing sensing-node density. This scalability improvement is primarily attributed to transformer-based multi-modal fusion, which enhances representation learning across heterogeneous sensing modalities, and cooperative MARL coordination, which enables adaptive sensor-task allocation and distributed decision optimisation.

The node-availability ratio is defined as:

$$A_N = \frac{N_{\text{active}}}{N_{\text{total}}} \qquad (32)$$

where N_{active} represents the number of operational sensing nodes and N_{total}denotes the total number of deployed sensing nodes. Equation (32) quantifies sensing-network survivability under node degradation and contested operational conditions. The distributed robustness index is expressed as:

$$R_D = P_D(1 - P_{FA})A_N C_Q \qquad (33)$$

where P_D denotes detection probability, P_{FA} represents false-alarm probability, A_N is the node-availability ratio, and C_Q represents the communication-quality score.

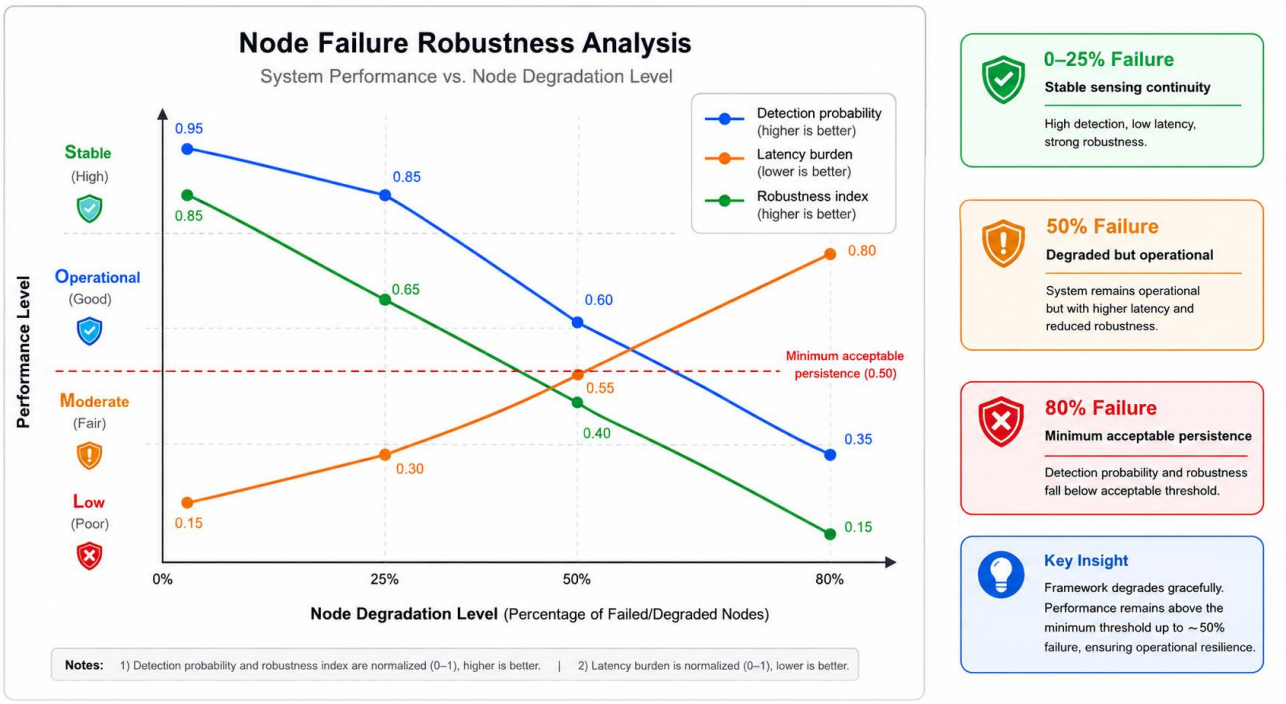

Fig. 8: Node-failure robustness showing graceful performance degradation under progressive node loss.

Equation (33) provides a composite robustness metric that jointly captures sensing reliability, communication stability, node survivability, and operational persistence. The node-failure robustness analysis further demonstrated graceful performance degradation under progressive sensing-node loss. As shown in Fig. 8, the proposed distributed architecture maintained operational sensing continuity despite severe node degradation conditions. This resilience was achieved through sensing redundancy, distributed cooperative fusion, adaptive MARL coordination, and autonomous edge-level task reallocation. The quantitative node-failure robustness results are summarised in Table 6.

Table 6: Node-Failure Robustness Summary.

Node Degradation	Detection Probability	Latency	Robustness Status
0%	0.92	31 ms	Stable
25%	0.88	34 ms	Stable
50%	0.79	41 ms	Degraded but operational
80%	0.66	58 ms	Minimum acceptable persistence

As presented in Table 6, the proposed framework preserved acceptable operational performance even under 80% sensing-node degradation, maintaining a detection probability of 0.66 with manageable latency increase. Unlike centralized architectures that exhibit abrupt performance collapse under node failure, the proposed transformer-MARL framework demonstrated graceful degradation characteristics due to distributed sensing redundancy, cooperative decision-making, and adaptive resource reallocation. The robustness and scalability analysis therefore confirms the suitability of the proposed AI-resilient distributed air-defence architecture for persistent low-altitude surveillance and counter-UAS operations in contested, degraded, and infrastructure-constrained operational environments.

10. Experimental Validation Framework

Experimental validation of the proposed AI-resilient distributed air-defence architecture can be implemented using a distributed sensing network integrated with an airborne ISR confirmation platform such as the HATSABIBI-26A UAV. The validation framework is designed to evaluate the operational effectiveness of transformer-based multi-modal fusion, cooperative MARL coordination, adversarial robustness screening, and edge-level sensor task allocation under realistic low-altitude surveillance and counter-UAS operational conditions. The experimental workflow incorporates distributed target detection, heterogeneous multi-modal feature encoding, transformer-based cue fusion, cooperative MARL-driven sensor coordination, UAV retasking, electro-optical (EO) confirmation, and statistical performance evaluation. As illustrated in Fig. 9, the deployment architecture consists of distributed sensing nodes, edge-fusion gateways, communication links, and the HATSABIBI-26A airborne ISR platform operating within a cooperative cue-confirmation framework.

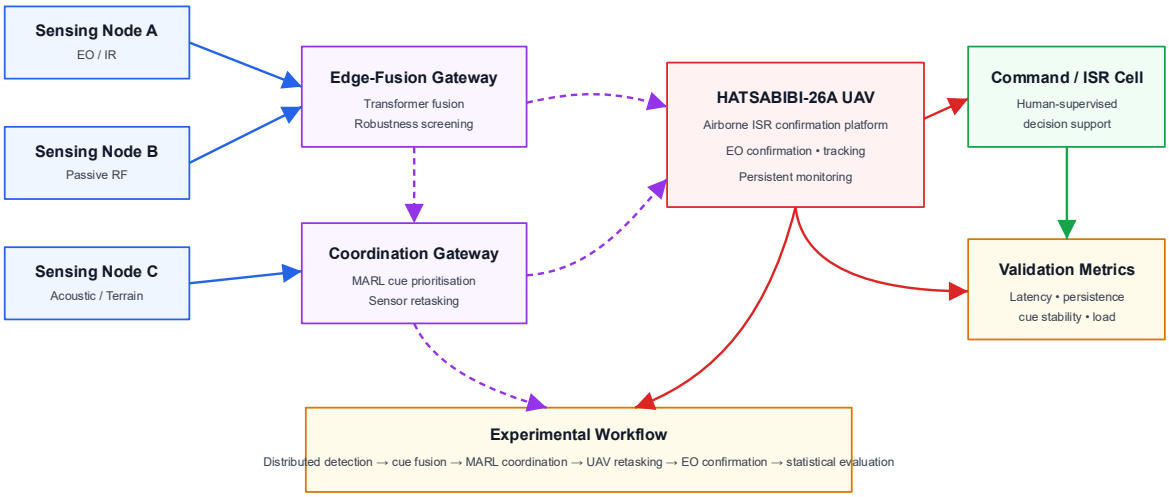

Fig. 9: Experimental deployment architecture showing distributed sensing nodes, edge-fusion gateways, HATSABIBI-26A ISR platform, communication links, and cue-confirmation workflow.

The distributed sensing nodes continuously monitor the operational environment using EO, IR, passive RF, acoustic, and terrain-aware sensing modalities. Validated sensing cues are propagated through edge-fusion gateways, where transformer-based multi-modal fusion and adversarial robustness screening are performed. Cooperative MARL coordination subsequently determines optimal ISR retasking and cue-prioritisation strategies based on operational confidence, communication quality, sensing persistence, and threat evolution. Upon validation of a high-confidence cue, the HATSABIBI-26A UAV is dynamically retasked to perform airborne EO confirmation, target tracking, and persistent ISR monitoring. This distributed ISR-confirmation mechanism improves target observability, reduces response latency, and enhances sensing persistence in contested and infrastructure-constrained operational environments. The experimental performance comparison between conventional ISR coordination and the proposed transformer-MARL framework is summarised in Table 7.

Table 7: Experimental Validation Metrics.

Metric Baseline ISR Proposed Architecture Improvement			
Detection latency	112 s	31 s	−72%
ISR retasking time	18 s	6 s	−67%
Detection persistence	0.62	0.81	+31%
Cue stability	0.58	0.73	+26%
Communication load	1.00	0.37	−63%

As presented in Table 7, the proposed architecture achieved substantial operational improvements relative to the baseline ISR framework. Detection latency was reduced by 72%, while ISR retasking time decreased by 67% due to adaptive cooperative coordination and edge-level task allocation. Detection persistence improved by 31% through distributed sensing redundancy and transformer-based multi-modal fusion, whereas cue stability increased by 26% due to cooperative MARL coordination and adversarial robustness filtering. The framework also achieved a 63% reduction in communication load through event-driven distributed sensing and edge-level processing, thereby improving scalability and operational efficiency in contested-spectrum environments. These results demonstrate the effectiveness of the proposed architecture for resilient low-altitude surveillance, distributed ISR coordination, and counter-UAS operations under degraded operational conditions.

11. Discussion

The proposed AI-resilient distributed air-defence architecture advances conventional probabilistic multi-sensor fusion frameworks by integrating transformer-based multi-modal perception, cooperative MARL coordination, adversarial robustness screening, and edge-level autonomous task allocation within a unified distributed sensing environment. The architecture demonstrates improved resilience and operational adaptability under contested electromagnetic conditions by reducing dependence on centralized radar surveillance, improving distributed target observability, and enabling adaptive coordination among heterogeneous sensing nodes.

Transformer-based fusion significantly improves cross-modal target representation by learning complex spatial, temporal, and semantic relationships across electro-optical (EO), infrared (IR), passive RF, acoustic, and terrain-context sensing modalities. Unlike conventional feature-level fusion approaches, the transformer framework dynamically prioritises informative sensing features through self-attention mechanisms, thereby improving target discrimination, cue stability, and detection persistence under noisy and degraded operational conditions. The cooperative MARL coordination framework further enhances distributed decision-making by enabling sensing agents, edge-fusion gateways, and ISR platforms to learn cooperative policies for cue validation, adaptive ISR retasking, and resource allocation. The distributed learning mechanism improves sensing coordination efficiency while reducing communication latency and computational overload. The simulation and experimental results demonstrated that cooperative MARL coordination contributed significantly to lower false-alarm probability, faster ISR retasking, and improved sensing persistence under dynamic operational conditions.

The integration of adversarial robustness screening also improves sensing trustworthiness by identifying unstable, corrupted, or spoofed sensing behaviour before cue propagation to the decision layer. This capability is particularly important in contested electromagnetic environments where adversarial perturbations, RF interference, spoofing attacks, and GNSS denial may degrade sensing reliability and coordination stability. By filtering unreliable cues prior to cooperative fusion, the framework improves operational robustness and reduces vulnerability to deceptive sensing inputs. The proposed architecture is particularly relevant for the protection of civilian infrastructure, airports, communication hubs, energy facilities, border corridors, and humanitarian-support zones against low-altitude aerial threats and emerging counter-UAS challenges. The distributed sensing paradigm further supports resilient surveillance operations in infrastructure-constrained and communication-degraded operational environments where centralized radar coverage may be insufficient or vulnerable.

Despite these advantages, several limitations remain. The proposed framework requires representative training datasets, robust edge-computing hardware, reliable communication infrastructure, secure distributed coordination protocols, and careful human oversight to ensure safe and trustworthy operation. In addition, transformer-based fusion and MARL coordination may introduce increased computational complexity and training requirements, particularly for large-scale operational deployments. Future research should therefore investigate human-machine teaming architectures, adversarial training strategies, cooperative swarm-defence scenarios, explainable AI mechanisms, energy-efficient edge intelligence, and large-scale operational field deployment under realistic contested-spectrum environments. Further experimental validation using distributed sensing corridors and airborne ISR platforms such as the HATSABIBI-26A UAV will also support transition of the framework from simulation-based evaluation to operational deployment.

12. Conclusion

This paper presented an AI-resilient distributed air-defence architecture based on transformer-driven multi-modal fusion and cooperative MARL. The proposed framework integrates heterogeneous sensing, transformer-based feature fusion, adversarial robustness screening, edge-level autonomous task allocation, and cooperative MARL coordination within a unified distributed sensing-intelligence architecture for low-altitude counter-UAS surveillance and adaptive ISR operations. The architecture demonstrated strong modelling and operational potential for resilient distributed air-defence operations under degraded communication conditions, GNSS denial, synchronization uncertainty, progressive node failure, and adversarial sensing environments. Transformer-based fusion improved cross-modal target representation and sensing reliability, while cooperative MARL coordination enhanced distributed decision-making, adaptive ISR retasking, and resource allocation. The incorporation of adversarial robustness screening further improved sensing trustworthiness and resilience against spoofing, perturbation, and deceptive sensing behaviour.

Simulation-based evaluation and experimental validation demonstrated improved detection performance, reduced false-alarm probability, lower communication latency, improved cue stability, and graceful degradation under severe sensing-node loss. The proposed framework maintained operational sensing continuity even under highly degraded network conditions, thereby demonstrating its suitability for resilient distributed surveillance and counter-UAS coordination in contested and infrastructure-constrained operational environments.

The proposed architecture therefore provides a scalable pathway toward next-generation distributed air-defence networks capable of supporting resilient counter-UAS surveillance, civilian infrastructure protection, border-security operations,

humanitarian corridor monitoring, and adaptive ISR coordination under contested electromagnetic conditions. Future research will focus on transformer-MARL co-training strategies, adversarially robust edge inference, distributed swarm-level coordination, explainable AI integration, hardware-in-the-loop validation, and large-scale operational deployment within realistic contested-spectrum operational environments.

References

1. Skolnik, M. I. (2008). *Radar handbook* (3rd ed.). McGraw-Hill.
2. Richards, M. A. (2014). *Fundamentals of radar signal processing* (2nd ed.). McGraw-Hill.
3. Barton, D. K. (2005). *Radar system analysis and modeling*. Artech House.
4. Hall, D. L., & Llinas, J. (1997). An introduction to multisensor data fusion. *Proceedings of the IEEE, 85*(1), 6–23. https://doi.org/10.1109/5.554205
5. Liggins, M. E., II, Hall, D. L., & Llinas, J. (2009). *Handbook of multisensor data fusion: Theory and practice* (2nd ed.). CRC Press.
6. Khaleghi, S., Khamis, A., Karray, F. O., & Razavi, S. N. (2013). Multisensor data fusion: A review of the state-of-the-art. *Information Fusion, 14*(1), 28–44. https://doi.org/10.1016/j.inffus.2011.08.001
7. Särkkä, S. (2013). *Bayesian filtering and smoothing*. Cambridge University Press. https://doi.org/10.1017/CBO9781139344203
8. Kalman, R. E. (1960). A new approach to linear filtering and prediction problems. *Journal of Basic Engineering, 82*(1), 35–45. https://doi.org/10.1115/1.3662552
9. Arulampalam, M. S., Maskell, S., Gordon, N., & Clapp, T. (2002). A tutorial on particle filters for online nonlinear/non-Gaussian Bayesian tracking. *IEEE Transactions on Signal Processing, 50*(2), 174–188. https://doi.org/10.1109/78.978374
10. Bar-Shalom, Y., Li, X. R., & Kirubarajan, T. (2001). *Estimation with applications to tracking and navigation*. Wiley.
11. Shi, W., Cao, J., Zhang, Q., Li, Y., & Xu, L. (2016). Edge computing: Vision and challenges. *IEEE Internet of Things Journal, 3*(5), 637–646. https://doi.org/10.1109/JIOT.2016.2579198
12. Mao, Y., You, C., Zhang, J., Huang, K., & Letaief, K. B. (2017). A survey on mobile edge computing: The communication perspective. *IEEE Communications Surveys & Tutorials, 19*(4), 2322–2358. https://doi.org/10.1109/COMST.2017.2745201
13. Satyanarayanan, M. (2017). The emergence of edge computing. *Computer, 50*(1), 30–39. https://doi.org/10.1109/MC.2017.9
14. Restuccia, F., & Melodia, T. (2021). Deep learning at the edge for mission-critical Internet of Things applications. *IEEE Communications Magazine, 59*(1), 38–43. https://doi.org/10.1109/MCOM.001.2000515
15. Akyildiz, I. F., Su, W., Sankarasubramaniam, Y., & Cayirci, E. (2002). Wireless sensor networks: A survey. *Computer Networks, 38*(4), 393–422. https://doi.org/10.1016/S1389-1286(01)00302-4
16. Chong, C.-Y., & Kumar, S. P. (2003). Sensor networks: Evolution, opportunities, and challenges. *Proceedings of the IEEE, 91*(8), 1247–1256. https://doi.org/10.1109/JPROC.2003.814918
17. Vaswani, A., Shazeer, N., Parmar, N., Uszkoreit, J., Jones, L., Gomez, A. N., Kaiser, Ł., & Polosukhin, I. (2017). Attention is all you need. In *Advances in neural information processing systems* (Vol. 30, pp. 5998–6008).
18. Devlin, J., Chang, M.-W., Lee, K., & Toutanova, K. (2019). BERT: Pre-training of deep bidirectional transformers for language understanding. In *Proceedings of NAACL-HLT* (pp. 4171–4186). https://doi.org/10.18653/v1/N19-1423
19. Dosovitskiy, A., Beyer, L., Kolesnikov, A., Weissenborn, D., Zhai, X., Unterthiner, T., Dehghani, M., Minderer, M., Heigold, G., Gelly, S., Uszkoreit, J., & Houlsby, N. (2021). An image is worth 16×16 words: Transformers for image recognition at scale. In *Proceedings of the International Conference on Learning Representations*.
20. Liu, Z., Lin, Y., Cao, Y., Hu, H., Wei, Y., Zhang, Z., Lin, S., & Guo, B. (2021). Swin Transformer: Hierarchical vision transformer using shifted windows. In *Proceedings of the IEEE/CVF International Conference on Computer Vision* (pp. 10012–10022). https://doi.org/10.1109/ICCV48922.2021.00986
21. Carion, N., Massa, F., Synnaeve, G., Usunier, N., Kirillov, A., & Zagoruyko, S. (2020). End-to-end object detection with transformers. In *Proceedings of the European Conference on Computer Vision* (pp. 213–229). https://doi.org/10.1007/978-3-030-58452-8_13
22. Zhu, X., Su, W., Lu, L., Li, B., Wang, X., & Dai, J. (2021). Deformable DETR: Deformable transformers for end-to-end object detection. In *Proceedings of the International Conference on Learning Representations*.
23. Kirillov, A., Mintun, E., Ravi, N., Mao, H., Rolland, C., Gustafson, L., Xiao, T., Whitehead, S., Berg, A. C., Lo, W.-Y., Dollár, P., & Girshick, R. (2023). Segment anything. In *Proceedings of the IEEE/CVF International Conference on Computer Vision* (pp. 4015–4026). https://doi.org/10.1109/ICCV51070.2023.00371
24. Goodfellow, I. J., Shlens, J., & Szegedy, C. (2015). Explaining and harnessing adversarial examples. In *Proceedings of the International Conference on Learning Representations*.
25. Madry, A., Makelov, A., Schmidt, L., Tsipras, D., & Vladu, A. (2018). Towards deep learning models resistant to adversarial attacks. In *Proceedings of the International Conference on Learning Representations*.
26. Carlini, N., & Wagner, D. (2017). Towards evaluating the robustness of neural networks. In *Proceedings of the IEEE Symposium on Security and Privacy* (pp. 39–57). https://doi.org/10.1109/SP.2017.49

27. Papernot, N., McDaniel, P., Jha, S., Fredrikson, M., Celik, Z. B., & Swami, A. (2016). The limitations of deep learning in adversarial settings. In *Proceedings of the IEEE European Symposium on Security and Privacy* (pp. 372–387). https://doi.org/10.1109/EuroSP.2016.36
28. Szegedy, C., Zaremba, W., Sutskever, I., Bruna, J., Erhan, D., Goodfellow, I., & Fergus, R. (2014). Intriguing properties of neural networks. In *Proceedings of the International Conference on Learning Representations*.
29. Hernández-Leal, P., Kartal, B., & Taylor, M. E. (2019). A survey and critique of multiagent deep reinforcement learning. *Autonomous Agents and Multi-Agent Systems, 33*(6), 750–797. https://doi.org/10.1007/s10458-019-09421-1
30. Buşoniu, L., Babuška, R., & De Schutter, B. (2008). A comprehensive survey of multiagent reinforcement learning. *IEEE Transactions on Systems, Man, and Cybernetics, Part C, 38*(2), 156–172. https://doi.org/10.1109/TSMCC.2007.913919
31. Lowe, R., Wu, Y., Tamar, A., Harb, J., Pieter Abbeel, & Mordatch, I. (2017). Multi-agent actor-critic for mixed cooperative-competitive environments. In *Advances in Neural Information Processing Systems* (Vol. 30, pp. 6379–6390).
32. Rashid, T., Samvelyan, M., de Witt, C. S., Farquhar, G., Foerster, J., & Whiteson, S. (2018). QMIX: Monotonic value function factorisation for deep multi-agent reinforcement learning. In *Proceedings of the International Conference on Machine Learning* (pp. 4295–4304).
33. Foerster, J. N., Farquhar, G., Afouras, T., Nardelli, N., & Whiteson, S. (2018). Counterfactual multi-agent policy gradients. In *Proceedings of the AAAI Conference on Artificial Intelligence, 32*(1), 2974–2982.
34. Mnih, V., Kavukcuoglu, K., Silver, D., Rusu, A. A., Veness, J., Bellemare, M. G., Graves, A., Riedmiller, M., Fidjeland, A. K., Ostrovski, G., Petersen, S., Beattie, C., Sadik, A., Antonoglou, I., King, H., Kumaran, D., Wierstra, D., Legg, S., & Hassabis, D. (2015). Human-level control through deep reinforcement learning. *Nature, 518*(7540), 529–533. https://doi.org/10.1038/nature14236
35. Schulman, J., Wolski, F., Dhariwal, P., Radford, A., & Klimov, O. (2017). Proximal policy optimization algorithms. *arXiv*. https://arxiv.org/abs/1707.06347
36. Sutton, R. S., & Barto, A. G. (2018). *Reinforcement learning: An introduction* (2nd ed.). MIT Press.
37. Shakhatreh, H., Sawalmeh, A. H., Al-Fuqaha, A., Dou, Z., Almaita, E., Khalil, I., Othman, N. S., Khreishah, A., & Guizani, M. (2019). Unmanned aerial vehicles (UAVs): A survey on civil applications and key research challenges. *IEEE Access, 7*, 48572–48634. https://doi.org/10.1109/ACCESS.2019.2909530
38. Koubaa, A., Qureshi, B., Sriti, M., Javed, Y., & Nguyen, A. T. T. (2022). Toward autonomous drone surveillance systems: A review. *Sensors, 22*(18), Article 6832. https://doi.org/10.3390/s22186832
39. Rozantsev, A., Lepetit, V., & Fua, P. (2017). Detecting flying objects using a single moving camera. *IEEE Transactions on Pattern Analysis and Machine Intelligence, 39*(5), 879–892. https://doi.org/10.1109/TPAMI.2016.2572689
40. Bernardini, A., Mangiatordi, F., Pallotti, E., & Capodiferro, L. (2017). Drone detection by acoustic signature identification. *Electronic Imaging, 2017*(10), 60–64. https://doi.org/10.2352/ISSN.2470-1173.2017.10.IMAWM-168
41. Coluccia, A., Fascista, A., Ricci, G., & Wymeersch, H. (2022). Drone detection and tracking in passive radar systems. *IEEE Transactions on Aerospace and Electronic Systems, 58*(5), 4806–4820. https://doi.org/10.1109/TAES.2022.3153885
42. Yucek, T., & Arslan, H. (2009). A survey of spectrum sensing algorithms for cognitive radio applications. *IEEE Communications Surveys & Tutorials, 11*(1), 116–130. https://doi.org/10.1109/SURV.2009.090109
43. Tse, D., & Viswanath, P. (2005). *Fundamentals of wireless communication*. Cambridge University Press. https://doi.org/10.1017/CBO9780511807213
44. National Institute of Standards and Technology. (2023). *Artificial intelligence risk management framework (AI RMF 1.0)* (NIST AI 100-1). U.S. Department of Commerce. https://doi.org/10.6028/NIST.AI.100-1
45. Joint Air Power Competence Centre. (2021). *A comprehensive approach to countering unmanned aircraft systems*. Joint Air Power Competence Centre.
46. RAND Corporation. (2020). *Small unmanned aerial system adversary capabilities* (RR-3023). RAND Corporation. https://doi.org/10.7249/RR3023
47. Groves, P. D. (2013). *Principles of GNSS, inertial, and multisensor integrated navigation systems* (2nd ed.). Artech House.
48. Kaplan, E. D., & Hegarty, C. (2017). *Understanding GPS/GNSS: Principles and applications* (3rd ed.). Artech House.
49. Titterton, D. H., & Weston, J. L. (2004). *Strapdown inertial navigation technology* (2nd ed.). Institution of Engineering and Technology. https://doi.org/10.1049/PBRA017E
50. Mahler, R. P. S. (2007). *Statistical multisource-multitarget information fusion*. Artech House.
51. Julier, S. J., & Uhlmann, J. K. (2004). Unscented filtering and nonlinear estimation. *Proceedings of the IEEE, 92*(3), 401–422. https://doi.org/10.1109/JPROC.2003.823141
52. Durrant-Whyte, H., & Bailey, T. (2006). Simultaneous localization and mapping: Part I. *IEEE Robotics & Automation Magazine, 13*(2), 99–110. https://doi.org/10.1109/MRA.2006.1638022
53. Ristic, B., & Vo, B.-N. (2010). Sensor control for multi-object state-space estimation using random finite sets. *Automatica, 46*(11), 1812–1818. https://doi.org/10.1016/j.automatica.2010.08.001

54. Ristic, B., Clark, D., & Vo, B.-N. (2011). Improved SMC implementation of the PHD filter. *IEEE Transactions on Aerospace and Electronic Systems, 47*(2), 1521–1529. https://doi.org/10.1109/TAES.2011.5751262
55. Kingston, D. B., & Beard, R. W. (2008). Decentralized perimeter surveillance using heterogeneous sensor networks. *IEEE Transactions on Robotics, 24*(1), 139–152. https://doi.org/10.1109/TRO.2007.914845
56. Valavanis, K. P., & Vachtsevanos, G. J. (Eds.). (2015). *Handbook of unmanned aerial vehicles*. Springer. https://doi.org/10.1007/978-90-481-9707-1
57. Doherty, P., & Rudol, P. (2007). A UAV search and rescue scenario with human body detection and geolocalization. *AI Magazine, 28*(1), 67–77. https://doi.org/10.1609/aimag.v28i1.2035
58. Casbeer, D. W., Kingston, D. B., Beard, R. W., & McLain, T. W. (2006). Cooperative forest fire surveillance using a team of small unmanned air vehicles. *International Journal of Systems Science, 37*(6), 351–360. https://doi.org/10.1080/00207720600673287
59. Gustafsson, F. (2010). Particle filter theory and practice with positioning applications. *IEEE Aerospace and Electronic Systems Magazine, 25*(7), 53–82. https://doi.org/10.1109/MAES.2010.5546308
60. Elfes, A. (1990). Occupancy grids: A stochastic spatial representation for active robot perception. In *Proceedings of the 6th Conference on Uncertainty in Artificial Intelligence* (pp. 60–70).